10.1098/rsta.2001.0808

THE ROYAL SOCIETY

Beyond simple depletion: phase behaviour of colloid–star polymer mixtures

By W. C. K. Poon[1], S. U. Egelhaaf[1], J. Stellbrink[1,2], J. Allgaier[2], A. B. Schofield[1] and P. N. Pusey[1]

[1]*Department of Physics and Astronomy, University of Edinburgh, Mayfield Road, Edinburgh EH9 3JZ, UK*

[2]*IFF-Neutronenstreuung II, Forschungszentrum Jülich GmbH, D-52425 Jülich, Germany*

Significant progress has been made in the last decade in understanding mixtures of hard-sphere colloids and (smaller) non-adsorbing, ideal, linear polymers. We introduce extra complexity into this simple model system by replacing the linear polymers with star-branched polymers with increasing functionality but constant radius of gyration. The observed phase diagrams, interpreted in light of what is known about hard-sphere colloid plus linear polymer and binary-hard-sphere mixtures, suggest that 32-arm stars are close to behaving hard-sphere-like in colloid–star mixtures at this size ratio.

Keywords: depletion; colloid; hard spheres; polymer; star polymer

1. Introduction

Colloids, polymers and surfactants almost always occur in the form of *mixtures*, whether in nature or as industrial products. One of the main tasks of soft condensed matter physics is to give generic (i.e. chemical-details-independent) insight into the structure, dynamics, phase behaviour and non-equilibrium properties of such mixtures. In practice, this entails identifying and studying in detail *model* systems stripped of as many extraneous features as possible.

Phase transitions in 'soft mixtures' can be driven mainly by enthalpy or entropy. Demixing in mixtures of polymers is the outstanding example of enthalpy-driven phenomena. In other cases, entropy dominates. Over the last decade, a system that has emerged as a model for such entropy-driven phase transitions is a mixture of hard-sphere colloids and (smaller) random-coil polymers in a near-theta solvent for the latter. In this system, the only interaction is that of excluded volume between the colloids and between the colloids and polymers; the polymer coils can be treated, to a first approximation, as ideal, and therefore interpenetrate each other freely.

Detailed studies by experiment, theory and simulation have led to substantial progress in understanding phase transitions and metastability in this idealized model. The essential physics is captured by the 'depletion' picture first proposed by Asakura & Oosawa (1958) and later independently by Vrij (1976). The centres of mass of polymer molecules are excluded from the vicinity of each particle, creating a 'depletion zone'. Overlap of the depletion zones from neighbouring particles creates extra volume for the polymers, thus increasing their entropy and lowering the free energy

of the system. It turns out that the topology of the equilibrium phase diagram depends on the relative sizes of the polymer and colloid. In addition, a rich 'zoo' of non-equilibrium behaviour has been identified and rationalized within an emerging general framework.

In this paper, we report experiments that go systematically beyond the idealized model: the nearly ideal linear polymer is replaced by star-branched polymers of increasing functionality (number of arms). To simplify the terminology, we will refer to the model system and the more complex systems just introduced as the colloid–polymer mixture and the colloid–star mixture, respectively. Moreover, when 'polymer' is used without qualification, it refers to a linear coil. Our generic aim is to see how far the emerging comprehensive understanding of colloid–polymer mixtures can aid the interpretation of phenomena in more complex systems. The specific motivation for choosing to study colloid–star mixtures is to observe the way star polymers of increasing functionality become progressively less like interpenetrable coils and more like mutually excluding hard particles (Seghrouchni *et al.* 1998). Thus, studying colloid–star mixtures with different functionalities can tell us how phase behaviour evolves between the extremes of a colloid–polymer mixture on the one hand, and a binary hard-sphere colloid on the other.

Below, we first review the phase behaviour and non-equilibrium properties of colloid–polymer mixtures in § 2. In § 3 we report the phase diagrams of colloid–star mixtures with stars of functionalities 2, 6, 16 and 32 but the same radii of gyration (thus maintaining a constant star-to-colloid size ratio). The data are then discussed in § 4 in terms of existing knowledge of colloid–polymer and binary hard-sphere mixtures. We conclude in § 5 with some speculations on colloid–star mixtures with stars of higher functionality, and suggestions of other areas of exploration that go systematically beyond simple depletion.

2. Colloid–polymer mixtures: a brief review

The theoretical prediction for the phase behaviour of a colloid–polymer mixture is by now well known (Gast *et al.* 1983; Lekkerkerker *et al.* 1992). The key parameter controlling the topology of the phase diagram is the ratio of the size of the polymer, e.g. as measured by its radius of gyration (r_g), to the radius of the colloid (R), $\xi = r_g/R$. When ξ is less than a certain critical value, ξ_c, the addition of polymer merely expands the fluid–crystal coexistence region of pure hard spheres, which occurs at $0.494 < \phi_c < 0.545$ (where ϕ_c is the colloid volume fraction). At $\xi > \xi_c$, a colloidal liquid phase becomes possible, and the phase diagram displays a colloidal gas–liquid critical point and a region of three-phase coexistence of colloidal gas, liquid and crystal. Mean-field theories predict $\xi_c \approx 0.33$. Computer simulations confirmed this picture (Meijer & Frenkel 1994; Dijkstra *et al.* 1999). The phase diagrams for $\xi = 0.1$ and 0.5 calculated according to Lekkerkerker *et al.* (1992) are shown in figure 1.

Experimentally, the most well-studied realization of this simple model system is a mixture of sterically stabilized PMMA spheres and linear polystyrene (PS) dispersed in *cis*-decahydronaphthalene (*cis*-decalin) (Ilett *et al.* 1995). These PMMA particles behave as nearly perfect hard spheres (Underwood *et al.* 1994), while *cis*-decalin is a theta-solvent for PS at 13 °C (Berry 1966). The qualitative picture outlined above was confirmed, although there were quantitative differences between experiment and theory. Experimentally, $\xi_c \approx 0.25$, and theory predicts concentrations of polymer in

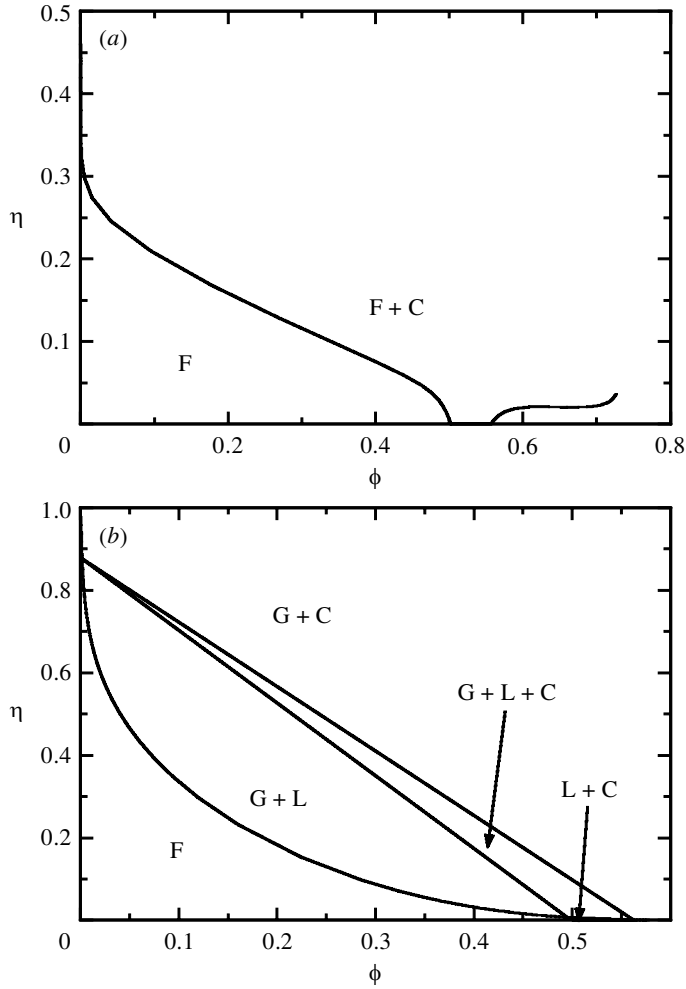

Figure 1. Theoretical phase diagrams of a mixture of non-adsorbing, ideal linear polymers (radius of gyration r_g) with hard spheres (radius R). The phase diagram topology depends on the size ratio $\xi = r_g/R$: (*a*) $\xi = 0.1$ and (*b*) $\xi = 0.5$. The horizontal and vertical axes are the colloid volume fraction, ϕ, and the polymer volume fraction, η (calculated using r_g), respectively. G denotes gas, L denotes liquid, F denotes fluid and C denotes crystal.

the dense colloidal phases that are too high by up to two orders of magnitude. The structure of the liquid phase in systems with $\xi \geqslant \xi_c$ has been measured (Moussaïd *et al*. 1999) and calculated (Louis *et al*. 1999; Dijkstra *et al*. 1999; Fuchs & Schweizer 2000).

The non-equilibrium behaviour of colloid–polymer mixtures has also been studied in detail. For all values of ξ studied, samples with the highest concentrations of polymer failed to phase separate according to the predictions of equilibrium theory, but produced 'transient gels': space-filling ramified networks of particles that collapse after finite time to give denser, amorphous sediments. The most well-studied transient gels (Poon *et al*. 1995; Evans & Poon 1997; Evans *et al*. 1997) are those formed in mixtures with small polymers, $\xi \sim 0.1$ or less. The formation and initial structure of

such gels have been discussed in terms of diffusion-limited cluster aggregation with finite bond energies (Haw *et al.* 1994, 1995*a*, *b*, 1997). The position of the gel line can be predicted with reasonable accuracy within the framework of mode-coupling theories of ergodicity breaking (Bergenholtz & Fuchs 1999). However, the long-time evolution and eventual collapse of these transient gels is still not fully understood (Poon *et al.* 1999*a*). Finally, the kinetic pathways followed by systems with $\xi > \xi_c$ phase separating into coexisting colloidal gas, liquid and crystal phases have also been identified and rationalized in terms of the 'free energy landscape' of the system (Poon *et al.* 1999*b*, 2000).

The literature of colloid–polymer mixtures is often cited in discussions of binary hard spheres with small ξ (say, 0.2 or less), now defined as the ratio of the radii of the two species of hard spheres $\xi = R_1/R_2$ (with $R_1 < R_2$). (We will use ξ to denote all size ratios in this paper; the meaning in each case should be clear from the context.) Published experimental phase diagrams at $\xi \sim 0.1$ disagree (see, for example, van Duijneveldt *et al.* 1993; Imhof & Dhont 1995; Dinsmore *et al.* 1995). Recent theoretical work (Louis *et al.* 2000*a*) suggests that this may reflect the extreme sensitivity of the phase behaviour to the form of the interaction between the two species, and therefore to the exact nature of the colloids used experimentally to model hard spheres. Small deviations from perfect hardness in the mutual interaction can be modelled as 'non-additivity'. The distance of closest approach of the centres of the two sphere species is given by

$$\sigma_{12} = (R_1 + R_2)(1 + \Delta), \tag{2.1}$$

where Δ is the non-additivity parameter. The ideal binary hard-sphere mixture corresponds to $\Delta = 0$, while the most extreme asymmetric non-additivity is that of the colloid–polymer mixture, where $R_1 = R$ is the radius of the colloid, $R_2 = 0$ for interpenetrable coils, and $\Delta = r_g/R \equiv \xi$. Louis *et al.* (2000*a*) found that small deviations of Δ from zero cause large shifts in phase boundaries. Within this framework but at the other extreme, Warren *et al.* (1995) have shown, using perturbative theory, that a small degree of non-ideality in the polymer does not affect the phase behaviour qualitatively (except possibly very near to $\xi = \xi_c$).

3. Experimental phase diagrams of colloid–star mixtures

Our specific motivation for studying star–colloid mixtures is to elucidate the role of depletant non-ideality. Equivalently, we want to understand the evolution of phase behaviour at constant size ratio as the non-additivity parameter evolves from $\Delta = \xi$ towards $\Delta = 0$. The polymer in a simple colloid–polymer mixture is close to ideal ($\Delta = \xi$). The most non-ideal possible second component is another hard sphere, giving a binary hard-sphere (BHS) mixture ($\Delta = 0$). Small degrees of non-ideality in the polymer can be induced by increasing the solvent temperature away from the theta point (Warren *et al.* 1995). To span the whole range from a colloid–polymer to a BHS mixture (i.e. $\Delta = \xi \to 0$), however, requires the use of star polymers (Seghrouchni *et al.* 1998).

Here we report experiments on a series of colloid–star mixtures in which the ratio of the radius of gyration of the stars, r_g, to the colloid radius, R, is kept approximately constant, $\xi = 0.5 \pm 0.01$, while the functionality is stepped through $f = 2$, 6, 16 and 32. The $f = 2$ system approximates to a simple colloid–polymer mixture. The colloids

are sterically stabilized PMMA spheres with radius $R = 104 \pm 3$ nm (determined by light scattering). The polymers have poly(butadiene) (PB) arms. These arms were synthesized by polymerizing butadiene with secondary butyl-lithium as initiator. The resulting polymer chains were coupled to chlorosilane linking agents having 6, 16 or 32 SiCl groups. The molecular weights of the PB arms were adjusted to give star polymers with values of r_g (determined by small-angle neutron scattering) as close to 50 nm as possible. The solvent is either *cis*-decalin or a mixture of this and tetralin (tetrahydronaphthalene) for index matching with the particles. In either case we have a good solvent for the stars (which is why the $f = 2$ system only *approximates* to a simple colloid–polymer mixture, where the polymer is ideal).

Mixtures as prepared were homogenized by extensive tumbling, and equilibrated and observed by eye at 25 °C. In all cases, the phase diagram has the same topology as that predicted for a colloid–polymer mixture with $\xi > \xi_c$ (cf. figure 1*b*). In particular, for colloid volume fractions $\phi_c \sim 0.1$–0.4, we observe successively, upon addition of stars, phase separation into coexisting colloid gas and liquid, triple coexistence of gas, liquid and crystal phases, and gas–crystal coexistence. At the highest star concentrations, transient gels were formed. The phase diagrams of the $f = 6$ and 32 mixtures are shown in figure 2, where the star concentration is given in terms of an effective volume fraction:

$$\phi_s = \tfrac{4}{3}\pi r_g^3 n_s. \tag{3.1}$$

Here n_s is the number density of stars.

Given the similarity of the topology of the phase diagram for all four mixtures, we will focus on the relative positions of the phase boundaries. We observe that the positions of all the phase boundaries in the (ϕ_c, ϕ_s)-plane drop as f increases. Figure 3*a* shows the three-phase (gas–liquid–crystal coexistence) regions for $f = 2$, 6, 16 and 32.

For comparison, we have also studied the phase behaviour of a BHS mixture at the same size ratio. The theoretical phase diagram for $\xi = 0.5$ was obtained earlier from extensive simulations (Eldridge *et al.* 1995). In our experiments, we used PMMA colloids with $R_1 = 256$ nm and $R_2 = 130$ nm dispersed in *cis*-decalin. Two types of superlattice structures, AB_2 and AB_{13} (where B is the smaller species) were observed, as well as crystals of the pure components (figure 4).

4. Discussion

A number of the significant features of the observed colloid–star phase diagrams can be discussed under a single heading: does an f-arm star behave more 'like' a (linear) polymer or a hard sphere when it is mixed with a hard-sphere colloid approximately twice its size? It turns out that for the highest functionality studied here, $f = 32$, this is a particularly intriguing question. The answer depends on exactly what kind of 'likeness' we seek, which suggests strongly that $f = 32$ is close to some 'cross-over functionality' as far as such mixtures are concerned.

(*a*) *Topology of the phase diagram*

The phase behaviour of any of the colloid–star mixtures is *qualitatively* different from that of the BHS mixture at the same size ratio. In all of the star–colloid mixtures, gas–liquid demixing is observed, while there is no such transition in the BHS

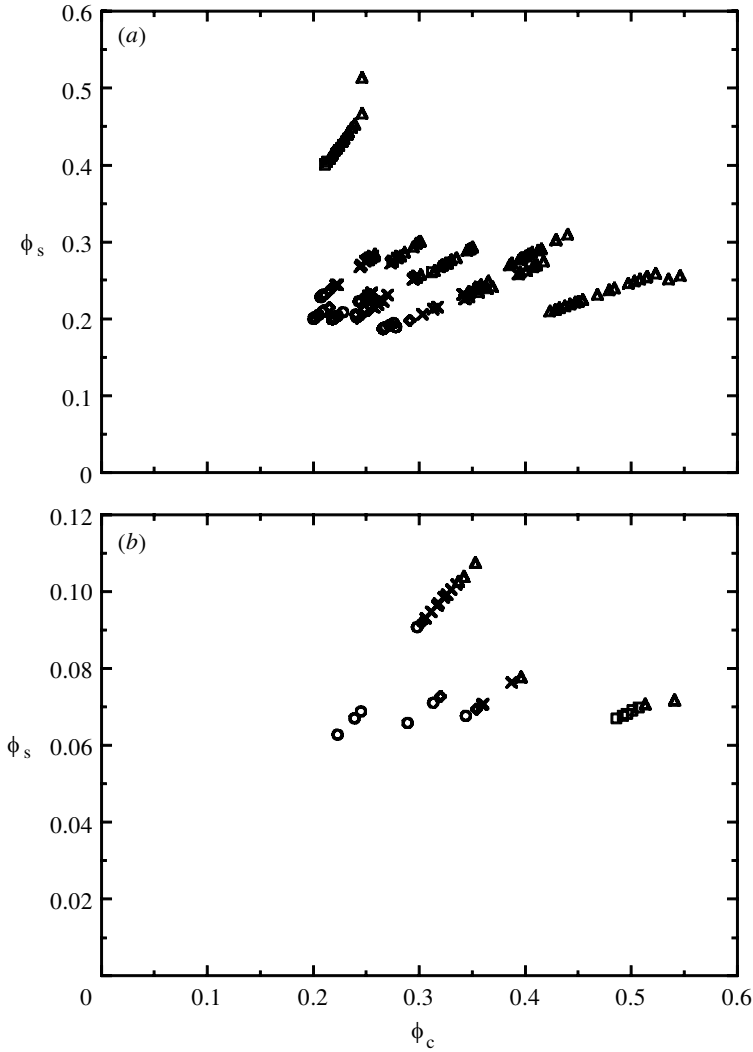

Figure 2. Phase diagrams of colloid–star mixtures: (*a*) $f = 6$, (*b*) $f = 32$. The horizontal and vertical axes are the colloid volume fraction, ϕ_c, and the star volume fraction, ϕ_s (calculated using r_g), respectively. The size ratio in both cases is $\xi = 0.5$; open circles denote single phase fluid, open diamonds denote gas–liquid coexistence, crosses denote gas–liquid–crystal coexistence, open squares denote fluid–crystal coexistence, and open triangles denote transient gel.

mixture. Thus, in this respect, stars with 6–32 arms behave as polymers and not as colloids.

However, while gas–liquid demixing occurs in each of the colloid–star mixtures we have studied, the area in the phase diagram occupied by the gas–liquid coexistence region clearly diminishes with increasing functionality. Figure 2 demonstrates this for the systems with $f = 6$ and 32. In the $f = 32$ mixture, gas–liquid demixing occurs in an almost vanishingly small strip in the phase diagram, while such samples are distributed over a finite area of the phase diagram in the $f = 6$ mixture. These observations imply that the stability of the liquid phase decreases with increasing

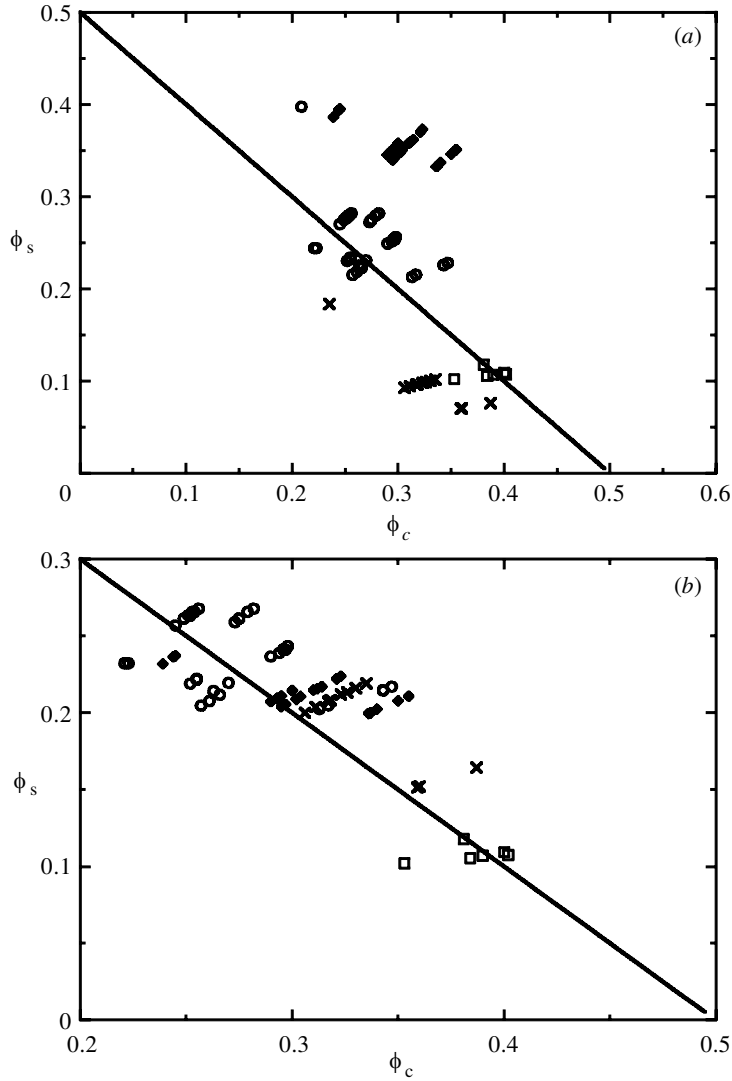

Figure 3. (*a*) Three phase-coexistence samples observed in colloid–star mixtures at $\xi = 0.5$ for various star functionalities. Filled diamonds represent the case where $f = 2$, open circles for $f = 6$, open squares for $f = 16$, and crosses for $f = 32$. Axes as in previous figure. (*b*) Scaled three-phase coexistence regions. The star volume fraction has been multiplied by 0.6, 0.95, 1 and 2.15 for the $f = 2$, $f = 6$, $f = 16$ and $f = 32$ data, respectively. The line in each case is the $\phi_{\mathrm{tot}} = \phi_{\mathrm{c}} + \phi_{\mathrm{s}} = 0.5$ contour.

depletant non-ideality, and suggest that colloid–star mixtures at $\xi \sim 0.5$ with star functionalities not much greater than 32 may show no gas–liquid demixing at all.

In principle, the discussion of gas–liquid coexistence and depletant non-ideality can be rendered more quantitative by appealing to the concept of non-additivity. However, in order to calculate the non-additivity parameter, Δ, defined in equation (2.1), we need to decide what values to use for the star–colloid interaction diameter and the star–star interaction radius (σ_{12} and R_2 in equation (2.1), respectively). It turns

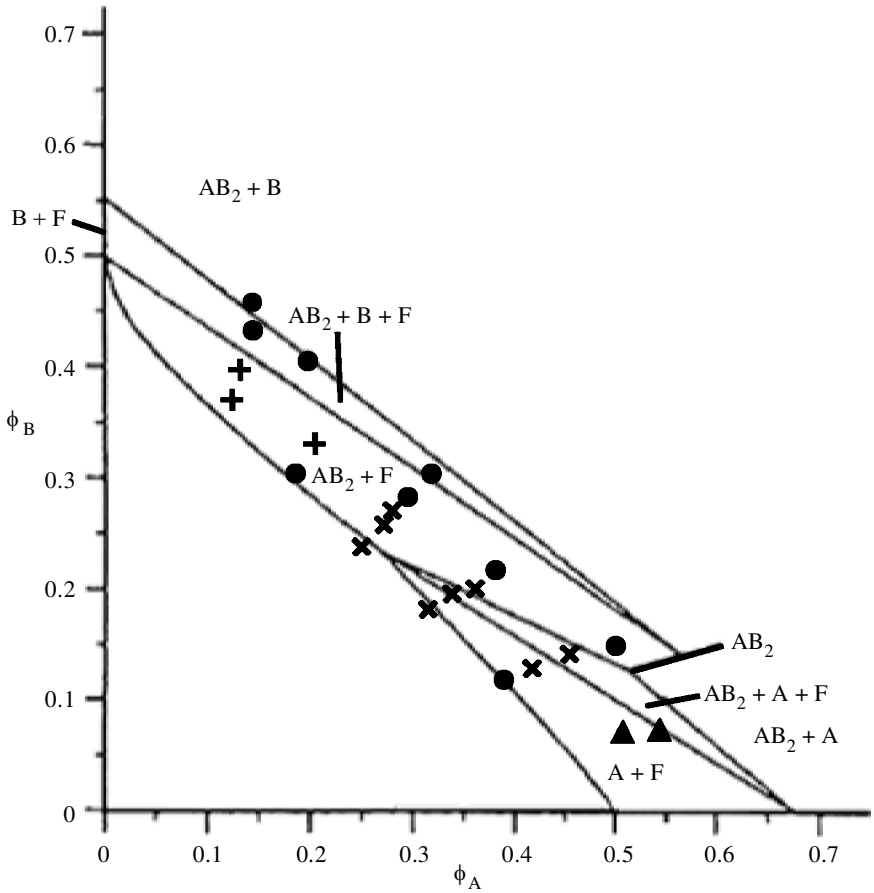

Figure 4. Phase diagram of a binary hard-sphere mixture at size ratio $\xi = 0.5$. ϕ_A and ϕ_B are the volume fractions of the large and small hard spheres, respectively. The points are experimental data. Filled circles represent the fluid or amorphous case, filled triangles the A crystal plus fluid case, crosses the AB_2 crystal plus fluid case, and pluses represent the AB_{13} crystal plus fluid case. The lines and labels correspond to the simulations of Eldridge *et al.* (1995).

out that the actual calculated value of Δ depends very sensitively on these parameters, slightly different choices may even switch its sign (A. Louis 2000, personal communication). Careful modelling of star–sphere and star–star interactions should be taken into account before such a discussion of star–colloid mixtures in terms of non-additive hard spheres can be attempted.

(*b*) *Crowding*

Another interesting feature of our results is that the ϕ_s needed to cause phase separation decreases significantly with increasing f, dropping by a factor of *ca.* 4 on going from $f = 2$ to $f = 32$. This is clearly illustrated in figure 3*a*.† Calculations of

† Given the narrowness of the gas–liquid region in all the star–colloid phase diagrams, we may take the position of the three-phase region to be a good indicator of the onset of phase separation in these systems.

the gas–liquid binodal based on a careful consideration of the pair potential between a star polymer and a spherical particle have been able to reproduce this feature (Dzubiella *et al.* 2001; see also Löwen *et al.*, this issue). Here we seek a qualitative understanding. Both experiment and theory show (figure 4) that phase separation of any kind is only observed in the BHS system if the overall volume fraction is greater than *ca.* 0.5. This is a generic feature for BHS mixtures with $0.5 \leqslant \xi \leqslant 0.625$ (Eldridge *et al.* 1995), and is intuitively plausible given that monodisperse hard spheres crystallize at $\phi_c = 0.494$. In other words, phase separation occurs whenever the system as a whole is 'crowded' enough. In figure 3*a*, we have plotted the $\phi_{tot} = \phi_c + \phi_s = 0.5$ contour. It seems that 32-arm stars are better at causing phase separation than hard spheres, while two-arm stars are worse at doing so. This is perhaps surprising, if we accept the clue from BHS mixtures that phase separation occurs whenever the whole system is crowded enough.

We are therefore prompted to revisit our definition of effective star volume fraction (equation (3.1)). Since the softness of the star–star and star–colloid interaction is expected to decrease with f (Löwen *et al.* 2000; Dzubiella *et al.* 2001), using r_g to calculate ϕ_s probably gives a poor measure of volume occupancy and therefore of crowding across systems with different functionalities. In fact, if we multiply ϕ_s by a factor of *ca.* 2.15 for the $f = 32$ mixture, then the onset of phase separation occurs almost exactly on the $\phi_{tot} = 0.5$ contour (figure 3*b*). Equivalently, as far as estimating 'crowding' is concerned, the correct radius to use is not r_g, but $(2.15)^{1/3} r_g$ for 32-arm stars. The factor of $(2.15)^{1/3}$ is very close to the ratio of the geometric radius to the radius of gyration for a homogeneous solid sphere (exact value $\sqrt{5/3}$). This suggests that as far as causing crowding in a mixture with hard-sphere colloids at the size ratio we have studied is concerned, we can treat a 32-arm star as a hard sphere with the same radius of gyration as the star.

Note that even our 32-arm star is very far from the 'all-core' limit. Based on a blob picture, Daoud & Cotton (1982) divided a star polymer into core, unswollen and swollen regions. The density is constant inside the core region. They showed that a star of functionality f made up of branches each having N statistical segments will be wholly core if $f \sim N^2$. We would certainly expect a star polymer at this limit to behave like a hard sphere. However, our 32-arm polymer has $N \sim 10^3$, and is thus very far from being 'all core' in the Daoud & Cotton sense.

The corresponding scaling factor to bring the $f = 2$ data down to the $\phi_{tot} = 0.5$ contour is $(0.6)^{1/3} \approx 0.85$ (figure 3*b*). A clue to why this factor is less than unity is found in the recent work of Louis *et al.* (2000*b*), who calculated the depletion potential between a hard wall and a linear polymer in a good solvent (modelled as a self-avoiding walk). The range of this depletion potential is significantly *smaller* than that predicted by using a simple geometric (Asakura & Oosawa 1958) model in which the polymers are ideal and excluded from the wall within a layer of thickness r_g. The corresponding calculation next to a curved interface has not yet been performed. Nevertheless, the hard-wall result gives us reason to expect that in so far as causing crowding is concerned, linear polymers in a good solvent behave as hard spheres with a radius smaller than their r_g.

For completeness, we note that previously published data for a colloid–polymer mixture in a very nearly theta solvent at size ratio $\xi = r_g/R = 0.57$ show phase separation starting to occur at almost exactly $\phi_{tot} = 0.5$ (see data in fig. 2(i) in Illett *et al.* 1995). This means that the 'crowding efficiency' of nearly ideal linear

polymers at this size ratio is well represented by the radius of gyration. That this is a reasonable conclusion can be demonstrated by calculating the exact free energy cost of immersing a hard sphere of radius R in a bath of ideal polymers of radius of gyration r_g. This is then equated to the free energy cost of immersing the same hard sphere in a sea of mutually non-interacting points that are excluded from coming closer than $\mathcal{R}$ to its surface. The limit of $R \to \infty$ (i.e. a hard wall) is well known: $\mathcal{R} = (2/\sqrt{\pi})r_g$. The calculations for general R have also been performed (A. Louis 2000, personal communication; see also Eisenriegler *et al.* 1996): $\mathcal{R}/r_g$ is a monotonically decreasing function of size ratio $\xi = r_g/R$, crossing unity at $\xi = 0.62$. This latter result explains the experimental observation that the 'crowding efficiency' for nearly ideal polymers with $r_g/R = 0.57$ can be estimated by their volume fraction calculated using the radius of gyration.

5. Conclusions

It is clear that star polymers with increasing functionality should behave less like linear coils and more like hard spheres. In this work, we have investigated this phenomenon in the context of star polymers causing phase separation when mixed with hard-sphere colloids at a fixed size ratio $\xi = r_g/R = 0.5$. In terms of the phase diagram topology, a 32-arm star plus hard-sphere colloid mixture behaves qualitatively like a simple colloid–polymer mixture. However, the gas–liquid coexistence region is very narrow, suggesting that it may vanish altogether at slightly higher star functionality. In terms of 'crowding efficiency', 32-arm stars behave like hard spheres with the same radius of gyration as the stars. These two observations together strongly suggest that colloid–star mixtures with $\xi = r_g/R = 0.5$ and $f > 32$ stars *may* show phase diagrams topologically equivalent to that of the BHS results reported in figure 4, opening up the intriguing possibility of colloid–star superlattice crystal structures. In this context, it may be significant that pure star polymers are predicted to crystallize when $f > 34$ (Löwen *et al.* 2000).

We conclude by returning to the title of the paper, 'Beyond simple depletion', and pointing out a number of other areas for exploration. It should be interesting to replace simple linear polymers with 'living polymers', e.g. worm-like micelles formed by surfactant self-assembly. Will these 'fragile' objects deplete hard spheres? Work in this direction is under way in our laboratory. While substantial literature exists for charged systems, comprehensive understanding is still lacking, partly because much of this literature predates recent work on the simple colloid–polymer mixtures reviewed in § 2. A systematic programme is called for using model components moving from charged particle–neutral polymer and neutral particle–charged polymer to a system in which both components are charged.

S.U.E. and A.B.S. thank Unilever Research and NASA, respectively, for financial support. J.S. is funded by the Deutsche Forschungsgemeinschaft. Discussions with Ard Louis and Hartmut Löwen concerning aspects of depletion, non-additivity and star physics have been very helpful.

References

Asakura, S. & Oosawa, F. 1958 *J. Polymer Sci.* **33**, 183–192.
Bergenholtz, J. & Fuchs, M. 1999 *Phys. Rev.* E **59**, 5706–5715.
Berry, G. C. 1966 *J. Chem. Phys.* **44**, 4550–4564.

Daoud, M. & Cotton, J. P. 1982 *J. Physique* **43**, 531–538.
Dijkstra, M., Brader, J. M. & Evans, R. 1999 *J. Phys. Condens. Matter* **11**, 10 079–10 106.
Dinsmore, A. D., Yodh, A. G. & Pine, D. J. 1995 *Phys. Rev.* E **52**, 4045–4057.
Dzubiella, J. *et al*. 2001 Phase separation in star polymer–colloid mixtures. (Submitted.)
Eisenriegler, E., Hanke, A. & Dietrich, S. 1996 *Phys. Rev.* E **54**, 1134–1152.
Eldridge, M. D., Madden, P. A., Pusey, P. N. & Bartlett, P. 1995 *Molec. Phys.* **84**, 395–420.
Evans, R. M. L. & Poon, W. C. K. 1997 *Phys. Rev.* E **56**, 5748–5758.
Evans, R. M. L., Poon, W. C. K. & Cates, M. E. 1997 *Europhys. Lett.* **38**, 595–600.
Fuchs, M. & Schweizer, K. S. 2000 *Europhys. Lett.* **51**, 621–627.
Gast, A. P., Hall, C. K. & Russel, W. B. 1983 *J. Colloid Interface Sci.* **96**, 251–267.
Haw, M. D., Poon, W. C. K. & Pusey, P. N. 1994 *Physica* A **208**, 8–17.
Haw, M. D., Sievwright, M., Poon, W. C. K. & Pusey, P. N. 1995*a* *Physica* A **217**, 231–260.
Haw, M. D., Sievwright, M., Poon, W. C. K. & Pusey, P. N. 1995*b* *Adv. Colloid Interface Sci.* **62**, 1–16.
Haw, M. D., Poon, W. C. K. & Pusey, P. N. 1997 *Phys. Rev.* E **56**, 1918–1933.
Ilett, S. M., Orrock, A., Poon, W. C. K. & Pusey, P. N. 1995 *Phys. Rev.* E **51**, 1344–1352.
Imhof, A. & Dhont, J. K. G. 1995 *Phys. Rev. Lett.* **75**, 1662–1665.
Lekkerkerker, H. N. W., Poon, W. C. K., Pusey, P. N., Stroobants, A. & Warren, P. B. 1992 *Europhys. Lett.* **20**, 559–564.
Louis, A. A., Finken, R. & Hansen, J.-P. 1999 *Europhys. Lett.* **46**, 741–747.
Louis, A. A., Finken, R. & Hansen, J.-P. 2000*a* *Phys. Rev.* E **61**, R1028–R1031.
Louis, A. A., Bolhuis, P. G., Hansen, J. P. & Meijer, E. J. 2000*b* *Phys. Rev. Lett.* **85**, 2522–2525.
Löwen, H., Watzlawek, M., Likos, C. N., Schmidt, M., Jusufi, A. & Denton, A. R. 2000 *J. Phys. Condens. Matter* **12**, A465–A469.
Meijer, E. J. & Frenkel, D. 1994 *J. Chem. Phys.* **100**, 6873–6887.
Moussaïd, A., Poon, W. C. K., Pusey, P. N. & Soliva, M. F. 1999 *Phys. Rev. Lett.* **82**, 225–228.
Poon, W. C. K., Pirie, A. D. & Pusey, P. N. 1995 *Faraday Disc.* **101**, 65–76.
Poon, W. C. K., Starrs, L., Meeker, S. P., Moussaïd, A., Evans, R. M. L., Pusey, P. N. & Robins, M. M. 1999*a* *Faraday Disc.* **112**, 143–154.
Poon, W. C. K., Renth, F., Evans, R. M. L., Fairhurst, D. J., Cates, M. E. & Pusey, P. N. 1999*b* *Phys. Rev. Lett.* **83**, 1239–1242.
Poon, W. C. K., Renth, F. & Evans, R. M. L. 2000 *J. Phys. Condens. Matter* **12**, A269–A274.
Seghrouchni, R., Petekidis, G., Vlassopoulos, D., Fytas, G., Semenov, A. N., Roovers, J. & Fleischer, G. 1998 *Europhys. Lett.* **43**, 271–276.
Underwood, S. M., Taylor, J. R. & van Megen, W. 1994 *Langmuir* **10**, 3550–3554.
van Duijneveldt, J. S., Heinen, A. W. & Lekkerkerker, H. N. W. 1993 *Europhys. Lett.* **21**, 369–374.
Vrij, A. 1976 *Pure Appl. Chem.* **48**, 471–483.
Warren, P. B., Ilett, S. M. & Poon, W. C. K. 1995 *Phys. Rev.* E **52**, 5205–5213.